

Transport of Polymeric Nanoparticle Gene Carriers in Gastric Mucus

Michelle Dawson,[†] Eric Krauland,[‡] Denis Wirtz,^{†,§} and Justin Hanes^{*,†,‡}

Departments of Chemical and Biomolecular Engineering, Biomedical Engineering, and Materials Science and Engineering, The Johns Hopkins University, Baltimore, Maryland

Nanoparticle transport through mucosal barriers is often restricted owing to mucoadhesion and the highly viscoelastic nature of mucus gels, which may limit efficient drug and gene delivery. We formulated sub-200 nm particulates from poly(D,L-lactic-co-glycolic) acid (PLGA) and the cationic surfactant dimethyldioctadecylammonium bromide (DDAB). Subsequently, anionic DNA was condensed to the surface to obtain gene carriers with transfection rates 50-fold higher than those of naked DNA *in vitro*. Using the method of multiple particle tracking (MPT), we measured the transport rates of dozens of individual PLGA-DDAB/DNA nanoparticles in real time in reconstituted pig gastric mucus (PGM) that possessed physiologically relevant rheological properties. The average transport rate of PLGA-DDAB/DNA nanoparticles was 10-fold higher than those of similar size polystyrene nanoparticles. Improved transport rates, stability in mucus, and ability to transfect cells make PLGA-DDAB/DNA nanoparticles candidates for mucosal DNA vaccines and gene therapy.

Introduction

Cationic polymeric microparticles have previously been shown to efficiently condense DNA, leading to noncytotoxic gene carriers capable of stable gene expression in small animal models following intramuscular injection (1–3). In these studies, the effective dosage of DNA was reduced from 1–2 mg to 1–10 μg , a result attributed to the reduced degradation of DNA (since encapsulation leads to DNA degradation) and the enhanced amount of DNA immediately available to induce an immune response.

Mucosal immunization is of considerable interest since gastrointestinal, nasal, respiratory, and vaginal mucosal tissues all drain to lymph nodes, leading to both local and distal immune responses (4). Thus, immunization of one mucosal surface can lead to long-term protective immune responses on all other mucosal surfaces. However, the effectiveness of cationic nanoparticles to deliver DNA to mucosal sites relies on the ability of these particles to cross mucosal barriers (5, 6).

The primary component of mucus is high molecular weight mucin glycoproteins, which form numerous covalent and noncovalent bonds with other mucin molecules and various constituents, including DNA, alginate, and hyaluronan (5). Reconstituted mucus formulated from pig gastric, human cervical, and tracheobronchial mucins display similar mucus structures, with large rod or fiberlike aggregates of 5 nm in diameter and 100–5000 nm in length (7). The condensed and complex microstructure of the mucus network gives rise to a highly viscoelastic gel, which significantly impedes the transport rates of large macromolecules and nanoparticles (8–10).

Immobilized nanoparticles are subject to bacterial and enzymatic degradation and may also be cleared from the body by normal mucus clearance mechanisms. Although clearance rates are anatomically determined, mucus turnover rates in the GI tract are estimated as between 24 and 48 h (7). In the lungs, clearance rates are dependent on the region of particle deposition; however, normal tracheal mucus velocities, albeit more rapid than mucus velocities in the peripheral lung, range from 1–10 mm/min and turnover times are less than 1 h (11). As a result, it is imperative that drug and gene carriers designed to deliver their payload to epithelial cells be capable of efficiently traversing mucus layers coating mucosal surfaces.

In this study, cationic polymeric nanoparticles were formulated from a biocompatible and biodegradable polymer (poly(D,L-lactic-co-glycolic) acid, PLGA), cationic surfactant (dimethyldioctadecylammonium bromide, DDAB) and DNA, leading to positively charged particles with average sizes <200 nm in diameter. These particles aggregated slightly upon addition to mucus solutions reconstituted from pig gastric mucin, whereas 200 nm carboxylated polystyrene (COOH-PS) particles did not. Despite this fact, PLGA-DDAB/DNA particles exhibited average transport rates 10-fold higher than those of COOH-PS particles in gastric mucus.

Materials and Methods

Materials. Poly(D,L-lactic-co-glycolic) (PLGA) (Medisorb High I.V. 54:46) was obtained from Alkermes (Cincinnati, OH), and 1,2-diacyl-palmitoyl-glycerol-3-phosphocholine (DPPC) was purchased from Avanti Polar Lipids (Alabaster, AL). Dimethyldioctadecylammonium bromide (DDAB), bovine serum albumin (BSA), pig gastric mucin (PGM), and deoxyribonucleic acid (DNA) (sodium salt, from salmon testes) were purchased from Sigma (St. Louis, MO) and used without further purification. 2,2,2-Trifluoroethanol (TFE) was purchased from

* To whom correspondence should be addressed. Ph: (410) 516-3484. Fax: (410) 516-5510. Email: hanes@jhu.edu.

[†] Chemical and Biomolecular Engineering.

[‡] Biomedical Engineering.

[§] Materials Science and Engineering.

Fluka (Milwaukee, WI). Plasmid DNA was extracted from *Escherichia coli* culture (strain DH5a, plasmid p43-clz1, kindly donated by Dr. Kam Leong, Johns Hopkins University) grown in freshly prepared Luria Bertani (LB) broth supplemented with 100 mg/mL ampicillin (Kodak Chemicals, Rochester, NY) using a Endo-free Qiagen Megaprep (Valencia, CA) and subsequently resuspended in sterile, deionized water. The plasmid p43-clz1 contains the Lac-Z gene under the human early-intermediate cytomegalovirus (CMV) promoter and also contains a gene for ampicillin resistance. All other solutions and reagents were of analytical grade and used without further purification.

Formulation of Cationic PLGA Nanoparticles.

Particles were prepared by a solvent extraction/precipitation method. PLGA (3 mg/mL) and DDAB (10 mg/mL) were dissolved in TFE separately. Subsequently, 3 mL of PLGA solution (9 mg PLGA) and 200 μ L of DDAB solution (2 mg DDAB) were combined and added dropwise to 8 mL of filtered distilled water stirring on a magnetic plate. Next, 100 μ L of 1 mg/mL salmon testes DNA in distilled water was added to the water/TFE mixture and stirred for 3 h on a magnetic plate to allow for TFE evaporation. The final formulation was 1.1% DNA to PLGA (w/w) and 5% DNA to DDAB (w/w). The nanoparticle suspension was then passed through a 1 μ m Watman syringe filter (Kent, UK) to remove large impurities and subsequently spun down for 75 min at $15,000 \times g$ and 4 $^{\circ}$ C using a Beckman-Coulter Avanti J-25 centrifuge (Fullerton, CA) to pellet nanoparticles. Spin conditions were carefully chosen as to not spin down cationic lipid/DNA particles. PLGA-DDAB/DNA nanoparticles were resuspended in distilled water and lyophilized or used directly for characterization or transport studies.

Nanoparticle Characterization. The size and surface morphology of the nanoparticles were examined by transmission electron microscopy. Nanoparticles in suspension were adsorbed to carbon-coated ionized Formvar grids, negatively stained with 2% uranyl acetate, and observed with Philips 420 transmission electron microscope (Eindhoven, Netherlands).

The size and ζ -potential of the nanoparticles were determined by dynamic light scattering and laser Doppler anemometry, respectively, using a Zetasizer 3000 (Malvern Instruments, Southborough, MA). Size measurements were performed at 25 $^{\circ}$ C at a scattering angle of 90 $^{\circ}$. Samples were diluted in 150 mM NaCl with or without pig gastric mucin (PGM) (final mucin concentration was 10 mg/mL). ζ -Potential measurements were performed according to instrument instructions with samples diluted in 150 mM NaCl with or without PGM (final mucin concentration was 2 mg/mL).

Gel electrophoresis (Mini-sub cell GT, Bio-rad, Hercules, CA) was used to verify the binding of DNA to particles and the necessity for cationic surfactants in the DNA adsorption process. Twenty microliters of sample was run on an ethidium bromide stained 1.0% agarose gel (70 V for 60 min) in TAE buffer (Tris-Acetate-EDTA).

Nanoparticle and Naked DNA Transfections with Lac-Z Reporter Gene. Cos-7 cells were obtained from American Type Culture Collection (ATCC, Rockville, MD) and maintained in Dulbecco's Modified Eagle's Medium (DMEM) (Gibco, BRL) containing 10% fetal bovine serum (Gibco, BRL, Invitrogen Co., Carlsbad, CA). Cells seeded at a density of 1.8×10^6 cells/cm 2 on 35-mm 6-well plates were transfected at 50–60% confluency with PLGA-DDAB/DNA nanoparticles or plasmid DNA alone (the concentration in all cases was maintained to yield 2.5

μ g DNA per well, or 0.26 μ g DNA/cm 2). Cells were harvested 48 h after transfection. β -Galactosidase activity and total protein content were assayed using the standard β -galactosidase spectrophotometric assay (12) and the manufacturer's given micro-well protocol for the BCA assay (Pierce Chemical Co., Rockford, IL), respectively. Reported values of β -galactosidase expression were normalized to the total protein content per sample well ($n = 3$).

The toxicity of PLGA-DDAB/DNA nanoparticles to Cos-7 cells was assayed using a propidium iodide nucleic acid stain (Molecular Probes, Eugene, OR). Cos-7 cells seeded at 1×10^6 cells/cm 2 were allowed to reach 60% confluency and then incubated with PLGA-DDAB/DNA nanoparticles, naked DNA, or PolyFect/DNA particles and harvested after 48 h. The PLGA-DDAB/DNA particle volume was adjusted to give final DNA amounts of 1.0, 2.5, and 5.0 μ g per well, and naked DNA and PolyFect/DNA concentrations were adjusted to result in a final DNA content of 2.5 μ g per well. Harvested cells were resuspended in 500 μ g/mL propidium iodide solution, which intercalates with DNA released from necrotic cells. The percentage of dead cells was assayed using flow cytometry. Adsorption and emission maxima for propidium iodide are 535 and 617 nm.

Reconstituted Pig Gastric Mucus (PGM). Mucus was formulated from 60 mg/mL PGM, 3.2 mg/mL DPPC, and 32 mg/mL BSA in sputum buffer (85 mM Na $^+$, 75 mM Cl $^-$, 20 mM Hepes, pH 7.4) (9). Mucus was mixed on a stir plate for 48 h at 4 $^{\circ}$ C and stored at -20° C (9).

Rheology and Confocal Microscopy. Rheological characterization of gastric mucus was performed with a strain controlled cone-and-plate rheometer (ARES-100, Rheometrics, Piscataway, NJ) as previously described (13, 14). Dynamic tests were performed at 25 $^{\circ}$ C, and buffer evaporation was eliminated using a vapor trap. We report the time-dependent in-phase component of the stress divided by the amplitude of applied oscillatory deformation of fixed frequency, $G'(\omega)$, the out-of-phase component, $G''(\omega)$, and the phase angle, $\phi = \tan^{-1}(G''/G')$. G and G' are also commonly referred to as the elastic and viscous moduli, respectively.

Confocal images of particles embedded in reconstituted mucus were captured with a Zeiss LSM 510 Meta laser scanning confocal microscope. Mucus was placed in a Biopetechs thermal regulated chamber (Biopetechs, Butler, PA) maintained at 37 $^{\circ}$ C. Three-dimensional images were reconstructed using Metamorph software (Universal Imaging Corp., West Chester, PA).

Nanoparticle Transport Rates in PGM with Multiple Particle Tracking (MPT). Trajectories of fluorescently labeled carboxylated polystyrene particles (COOH-PS; Molecular Probes; -5 mV ζ -potential at pH 6; 200 nm diameter) and PLGA-DDAB/DNA nanoparticles with condensed salmon testes DNA (35 mV, 196 ± 29 nm diameter) in reconstituted PGM were recorded using a silicon-intensified target camera (VE-1000, Dage-MTI, Michigan, IN) mounted on an inverted epifluorescence microscope equipped with 100X oil-immersion objective (numerical aperture 1.3). The trajectories of $n = 109$ COOH-PS and $n = 120$ PLGA-DDAB/DNA particles were tracked in PGM samples contained within a microscope chamber maintained at 37 $^{\circ}$ C.

The centroid of each particle was tracked with 5 nm spatial resolution, determined by tracking the apparent displacements of microspheres immobilized on a glass microslide with a strong adhesive (15). Nanoparticle motion was tracked in 2-D by following the motion of

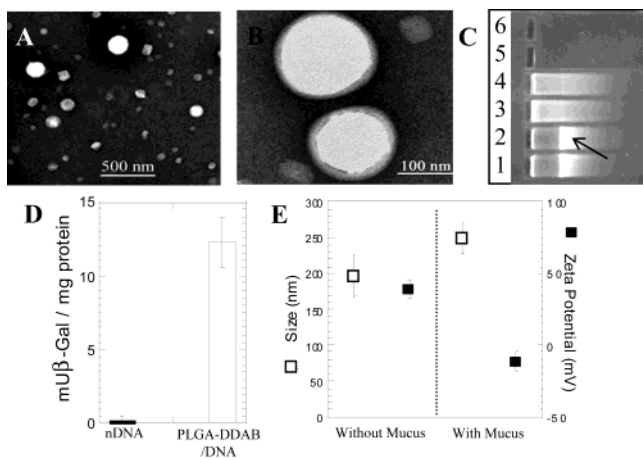


Figure 1. Characterization of PLGA-DDAB/DNA nanoparticles. (A, B) Transmission electron micrographs showed nanoparticle sizes <300 nm. (C) Complexation of salmon testes DNA with cationic PLGA-DDAB nanoparticles was assayed by UV gel electrophoresis. Lanes 1 and 2: free DNA (arrow shows primary band ~ 2 kb). Lanes 3 and 4: PLGA-DNA (no DDAB). Lanes 5 and 6: PLGA-DDAB/DNA nanoparticles. (D) PLGA-DDAB/DNA nanoparticles transfect Cos-7 cells with 50-fold increase in transfection efficiency compared to naked DNA. (E) The size and ζ -potential of PLGA-DDAB/DNA nanoparticles were assayed in 150 mM NaCl and in PGM. Size values represent the average value from 10 measurements, while the ζ -potential values were an average of three measurements ($n = 2$ separate batches).

nanoparticles in the plane of focus. For 2-D displacements to accurately represent 3-D motion, the fluid must be locally isotropic but need not be homogeneous (14). Images of the microspheres were captured with a custom routine incorporated in the Metamorph software (Universal Imaging Corp.) at a frequency of 30 Hz for 20 s, which gives a temporal resolution of 33 ms. The coordinates of nanoparticle centroids were transformed into families of time-averaged mean squared displacements (MSD), $\langle \Delta r^2(\Delta t) \rangle = \langle [x(t + \Delta t) - x(t)]^2 + [y(t + \Delta t) - y(t)]^2 \rangle$ ($\Delta t =$ time scale or time lag), from which distributions of MSDs and time-dependent particle diffusion coefficients ($D(\Delta t) = \langle \Delta r^2(\Delta t) \rangle / 4\Delta t$) were calculated as previously demonstrated (16). Diffusion coefficients were normalized with the theoretical diffusion coefficient of 200 nm particles in water as determined by the classical Stokes–Einstein equation.

Results and Discussion

Cationic microparticles with DNA adsorbed to their surfaces have been shown to efficiently transfect cells in vitro (1–3, 17). However, obtaining high transfection efficiencies in vivo is often limited by particle transport through extracellular barriers, including the mucosal barrier, which has been described as the foremost barrier to transfection in mucus-covered cells (5, 18, 19). To determine if cationic nanoparticles formulated from PLGA and DDAB with condensed DNA may be effective gene carriers for administration to mucosal sites, we produced PLGA-DDAB/DNA nanoparticles and studied their transport rates in reconstituted pig gastric mucus (PGM). Reconstituted PGM was found to have compositional and rheological properties physiologically relevant to gastrointestinal (GI), nasal, and respiratory mucus (7).

PLGA-DDAB/DNA Nanoparticle Characterization. PLGA-DDAB/DNA nanoparticles with sizes less than 200 nm (Figure 1A and B) can be designed to tightly bind DNA with high efficiency (Figure 1C). In addition, their small size compared to previous cationic particles

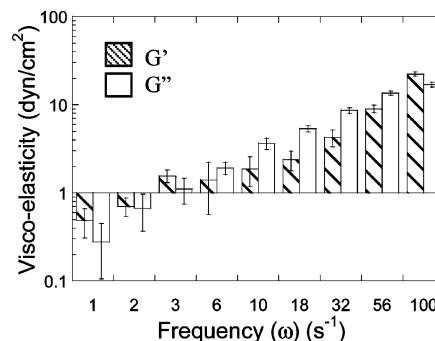


Figure 2. Elastic (G') and viscous (G'') moduli of reconstituted pig gastric mucus ($n = 3$). Note that at low frequencies PGM acts more elastic than viscous, with phase angle, $\phi = \tan^{-1}(G''/G') \sim 30^\circ$, but it yields at low frequency (2.5 s^{-1}) and the phase angle shifts to $\phi \sim 50^\circ$.

in the micron-range (1–3, 17) allows them to enter cells, either through nonspecific or receptor-mediated endocytosis. Similar to the results that Singh found with cationic microparticles (1, 2), the transfection efficiency of PLGA-DDAB/DNA nanoparticles was 50-fold higher than that of naked DNA (Figure 1D). At the concentration used in the transfection study, PLGA-DDAB/DNA nanoparticles ($16.6 \pm 6.2\%$ dead cells) were less toxic than PolyFect/DNA particles containing the same amount of DNA ($23.9 \pm 1.2\%$ dead cells) but more toxic than naked DNA alone ($4.7 \pm 2.4\%$ dead cells). The toxicity of PLGA-DDAB/DNA nanoparticles showed a dose-dependency with slightly lower particle concentrations (corresponding to $1 \mu\text{g}$ DNA total, or 2.5-fold lower concentration than used in the transfection study) resulting in background levels of cell toxicity ($7.2 \pm 0.6\%$ dead cells, not significantly different than naked DNA controls). Singh and co-workers reported that PLGA-DDAB/DNA microparticles caused no acute toxicity with particle doses resulting in the equivalent of 1 mg of DNA per animal (guinea pig) (1).

Incubation of PLGA-DDAB/DNA nanoparticles in mucus for <30 min changed the average particle surface charge from 39 ± 6 mV to -11 ± 7 mV, and the average particle size increased from 196 ± 29 nm to 249 ± 21 nm. The change in size and surface charge of PLGA-DDAB/DNA particles indicated that mucus constituents adsorbed on particle surfaces, leading to a significant increase in particle diameter.

Rheological Characterization of PGM. The highly viscoelastic properties and gel formation of mucus (phase angle $<45^\circ$) arise primarily from the high molecular weights and expanded conformations of mucin glycoproteins in aqueous solution. The ability of mucus to undergo gelation is also strongly affected by the concentrations of lipids and macromolecules, which noncovalently interact with mucins promoting the formation of larger mucin fibers that overlap to form dense mucus networks (20, 21). Physiologically, the high viscoelasticity of mucus gels is maintained to provide a barrier to microbial and particle transport; high elasticity also allows mucus to be engaged by ciliated cells or moved by pulsatory forces as it is cleared from the body (20). The viscous and elastic properties are properly matched in vivo to achieve appropriate mucus clearance rates (5, 20).

The frequency-dependent elastic and viscous moduli were used to characterize the viscoelastic nature of reconstituted pig gastric mucus (PGM) used in this study (Figure 2). The phase angle of the reconstituted mucus ($\phi = \tan^{-1}(G''/G') = 30^\circ$ at $\omega = 1 \text{ s}^{-1}$) showed that the viscosity and elasticity of PGM were matched similarly to physiological mucus (21). At low frequencies, PGM had

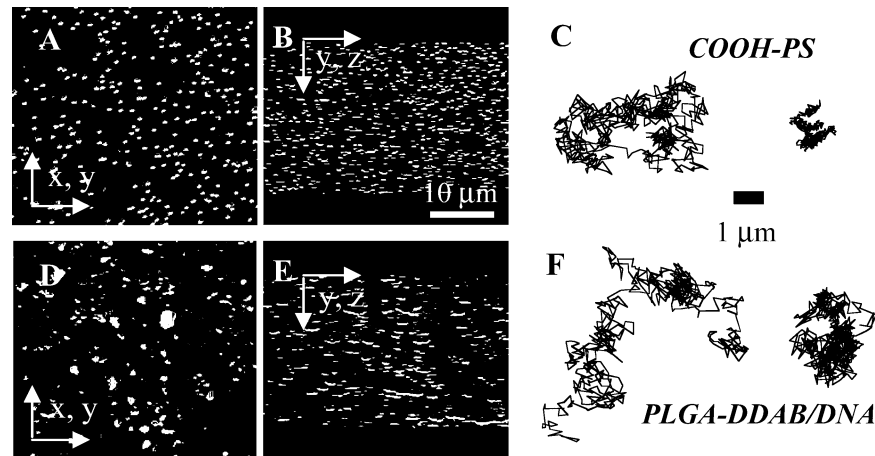


Figure 3. Reconstructed 3-D confocal images of fluorescently labeled (A, B) COOH-PS (note the uniform size and distribution) and (D, E) PLGA-DDAB/DNA nanoparticles (particle size is less uniform with aggregates). Diffusive and sub-diffusive 20-s trajectories of (C) COOH-PS and (F) PLGA-DDAB/DNA nanoparticle motion in PGM.

strong gel-forming properties, but gelation was disrupted at shear rates corresponding to a frequency of $\omega = 2.5 \text{ s}^{-1}$. Reconstituted mucus deforms at lower shear rates than crude mucus (21). However, particle transport studies are performed on quiescent fluids in this work, and thus, mucus is not subjected to deforming shear conditions.

PLGA-DDAB/DNA and 200 nm COOH-PS Nanoparticles Embedded in PGM. Following incubation in mucus, the ζ -potential measured for carboxylated polystyrene (COOH-PS) particles (-17.5 mV at pH 6) was close to that for PLGA-DDAB/DNA nanoparticles ($-11 \pm 7 \text{ mV}$ at pH 6), even though the initial ζ -potentials of the two particle types were quite different prior to incubation with mucus (39 ± 6 for PLGA-DDAB/DNA and -5 mV for COOH-PS). This result suggests that mucus components readily adsorb to the surface of each type of particle within minutes of their addition to mucus.

Confocal microscopy was used to collect three-dimensional images of nanoparticles embedded in reconstituted PGM samples (bead solution was $\sim 3\%$ total volume) (Figure 3A, B, D, and E). COOH-PS nanoparticles showed reduced aggregation when compared to PLGA-DDAB/DNA nanoparticles, which indicated that PLGA-DDAB/DNA nanoparticles were either adhering as clumps to mucin fibers or aggregating via particle-particle interactions mediated by mucus. Adhesion to mucus may not be surprising since DDAB, which remains on the surface of PLGA-DDAB/DNA nanoparticles, is a cationic surfactant and mucin and other macromolecules found in PGM are strongly anionic (22). Note that although COOH-PS particles did not appear to aggregate heavily in mucus, they may still be adherent to mucus as individual particles (see next section).

Nanoparticle Transport Rates Measured with Multiple Particle Tracking (MPT). The mobility of COOH-PS and PLGA-DDAB/DNA nanoparticles in PGM was tracked in real time in two-dimensions. Suggesting 2-D tracking represents the 3-D mobility of particles assumes that mucus is an isotropic fluid but not necessarily homogeneous. We verified with 3-D confocal microscopy that PLGA-DDAB/DNA and COOH-PS particle distributions in mucus are independent of location within the gel in the x , y , and z directions (Figure 3).

Twenty-second trajectories of nanoparticle motion in PGM showed that PLGA-DDAB/DNA nanoparticles appeared to be considerably more mobile than COOH-PS nanoparticles (Figure 3C and F). Individual particle

MSDs were used to determine the average (or “ensemble-average”) MSD, allowing the variation in particle transport rates with respect to time to be directly computed. The ensemble MSD of PLGA-DDAB/DNA nanoparticles was 10-fold higher than the ensemble MSD of 200 nm COOH-PS nanoparticles over a range of time scales (Figure 4A). Furthermore, the ensemble MSD of PLGA-DDAB/DNA nanoparticles had an almost linear dependency on time, indicating that the average transport rate in PGM was dominated by diffusive carriers. Nevertheless, particle motion is severely limited by the viscoelastic nature of PGM, as indicated by the normalized average (or “effective”) diffusion coefficients, which are 50- to 500-fold lower than their theoretical diffusivities in water (Figure 4B). The normalized diffusion coefficients show that the average particle transport rate decreases slightly with respect to time (Figure 4B), which would be expected, for example, if a significant fraction of particles underwent sub-diffusive transport (for example, particles adherent to mucus fibers).

The observation that PLGA-DDAB/DNA particles moved faster on average than COOH-PS particles was somewhat counterintuitive since PLGA-DDAB/DNA nanoparticle aggregation was expected to reduce their transport rates. Therefore, to further elucidate the mode and rate of particle transport in PGM, we examined the distributions of individual particle MSDs (Figure 5). The mode of transport of each individual particle was determined by the slope of the particle MSD versus time on a log-log scale. A slope of <1 indicated that transport was sub-diffusive, or hindered, whereas a slope of ~ 1 indicated that transport was diffusive. For time scales $<1 \text{ s}$, COOH-PS nanoparticle MSDs were primarily sub-diffusive (Figure 5A), indicating that a majority of these particles (101 of 109, or 93%, at time scales between 0.1 and 1 s) are transiently adherent to mucus or are temporarily trapped within cages formed by mucus fibers. In contrast, considerably more PLGA-DDAB/DNA nanoparticles had diffusive MSDs at earlier time scales (Figure 5B), with only 78% (94 of 120) undergoing sub-diffusive transport at time scales between 0.1–1 s. Therefore, although a considerable fraction of PLGA-DDAB/DNA particles appear to aggregate in PGM, a significantly higher percentage of PLGA-DDAB/DNA particles (22%) undergo diffusive transport at early time scales compared to COOH-PS particles (7%).

To quantify the degree of heterogeneity in particle transport rates, the distributions of the individual MSDs

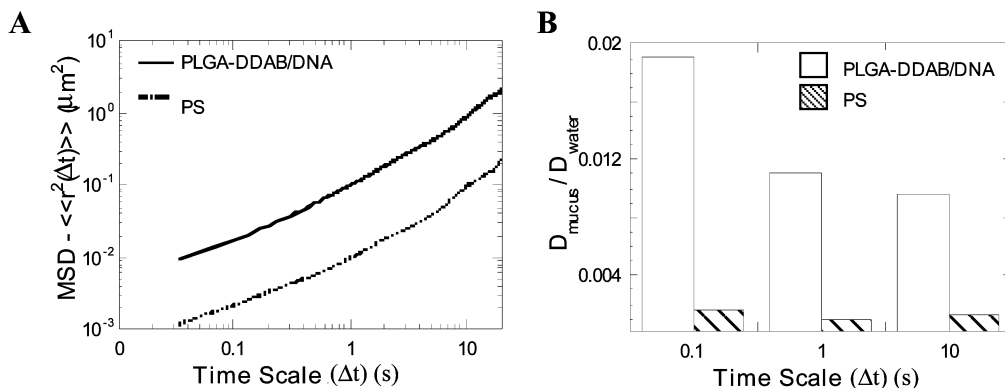


Figure 4. (A) Ensemble MSD of PLGA-DDAB/DNA and COOH-PS nanoparticles in PGM. (B) The average diffusion coefficients, normalized with the theoretical diffusivity of 200 nm particles in water, of COOH-PS and PLGA-DDAB/DNA show slight time dependence.

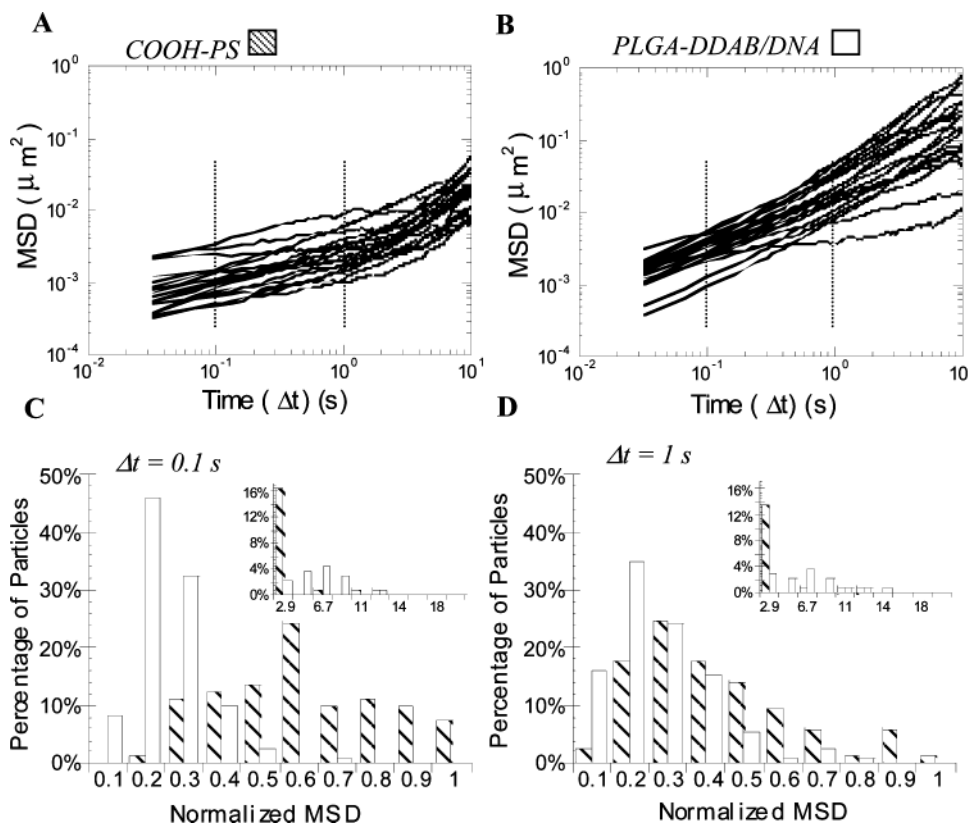


Figure 5. Twenty time-dependent particle MSDs for (A) COOH-PS and (B) PLGA-DDAB/DNA nanoparticles, randomly selected ($n = 109$ and 120 , respectively). The distribution of MSDs for COOH-PS (hatched bars) and PLGA-DDAB/DNA (open bars) particles, normalized with their respective ensemble averaged MSD, at (C) $\Delta t = 0.1$ s and (D) $\Delta t = 1$ s indicate that the majority of particles have MSDs less than the average. Note that a small percentage of faster particles largely affects the average rate of transport (see insets), especially at small time scales when many particles are moving with more sub-diffusive transport rates.

of COOH-PS and PLGA-DDAB/DNA nanoparticles at time scales of $\Delta t = 0.1$ and 1 s were normalized by their respective ensemble average MSDs (Figure 5C and D). In general, the mean MSD of each particle type was significantly smaller than the ensemble average MSD, indicating that a small percentage ($\sim 10\%$) of the particles contributed significantly to the average rate of transport. At early time scales ($\Delta t = 0.1$ s), when transport of COOH-PS nanoparticles was primarily sub-diffusive, the mean of the MSD was only 2-fold lower than the average; at larger time scales ($\Delta t = 1$ s), the mean was nearly 5-fold lower than the average. In contrast, for all time scales, PLGA-DDAB/DNA nanoparticles had mean transport rates that were 5-fold lower than the average. This result provided further evidence that a high percentage

of COOH-PS nanoparticles were either transiently adherent to mucus or temporarily trapped in microscopic cages in PGM over short time scales (thereby leading to a more homogeneous distribution of transport rates). Given time, some COOH-PS particles could resume diffusion by desorbing or escaping their sub-diffusive cages (leading to an increase in the heterogeneity of the particle transport rates). On the other hand, a higher number of PLGA-DDAB/DNA nanoparticles had diffusive transport rates at short time scales, leading to high heterogeneity in particle transport rates, but fewer changed their mode of transport over time, which was apparent in the similarities of the mean MSD at time scales of $\Delta t = 0.1$ and 1 s. This result suggests that, following the adhesion of a fraction of the PLGA-DDAB/

DNA particles, a significant percentage of the remaining particles were able to undergo unrestricted diffusive transport. Heterogeneities in particle transport rates may be important in assessing the efficiency of particles in traversing the mucosal barrier since gene delivery may only require a small percentage of gene carriers to reach target epithelial cells (5).

There are several possible explanations for the more rapid transport of the slightly aggregated (and thus, larger) PLGA-DDAB/DNA particles compared to COOH-PS particles. For example, Olmsted and co-workers (10) demonstrated that herpes simplex virus (HSV) particles adhere to mucin fibers found in cervical mucus, causing the fibers to collapse into coil-like structures and inducing the formation of larger pores around the condensed mucus. The rearrangement of the mucus network promoted more rapid local transport of HSV particles (10). Similarly, the observed PLGA-DDAB/DNA particle aggregates with mucus may have led to larger pores that promoted more rapid transport of PLGA-DDAB/DNA particles compared to COOH-PS particles. This hypothesis is supported indirectly by the fact that a considerably higher percentage of PLGA-DDAB/DNA nanoparticles (8.5%) exhibited a MSD greater than 5-fold of their ensemble average MSD compared to only 2.9% for COOH-PS nanoparticles, each at a time scale of 0.1 s (7.7% versus 3.9% at a time scale of 1 s for PLGA-DDAB/DNA versus COOH-PS, respectively).

A second possible explanation for the increased transport rates of PLGA-DDAB/DNA nanoparticles compared to those of the slightly smaller COOH-PS nanoparticles may be related to the difference in surface chemistries of the two particle types. PLGA-DDAB/DNA nanoparticle surfaces are coated with DNA, making them relatively hydrophilic compared to COOH-PS nanoparticles. Mucus is composed of a dense network of fibers that are relatively hydrophobic compared to the solution contained within the network pores. Therefore, it is possible that the fraction of PLGA-DDAB/DNA nanoparticles that do not interact electrostatically with negatively charged mucin glycoproteins are capable of enhanced transport in the hydrophilic mucus pores compared to COOH-PS particles, a larger fraction of which may adhere as single particles to the mucus network. This hypothesis is supported by the finding that a larger fraction of COOH-PS particles undergo sub-diffusive, or hindered, transport compared to PLGA-DDAB/DNA particles (Figure 5). The fact that each particle type appears to adsorb mucus components (as indicated by the decrease in ζ -potential for each particle upon incubation in mucus) presumably makes the particle surfaces more similar. If the entire surface is coated by mucus components, then the differences in initial surface chemistries may not be important, thus favoring the former hypothesis. Future studies aimed at quantifying the effects of particles on the pore structure of the mucus mesh and at determining the surface composition of the particles following incubation in mucus should help explain the transport phenomena observed.

Conclusions

Multiple particle tracking (MPT) was used to study transport rates of individual gene carriers in gastric mucus. Advantages of MPT include the ability to study individual particle transport and distributions of transport rates, as well as their contributions to the average or "bulk" properties, in complex biological environments (14, 23). We measured transport rates of cationic nanoparticles made from PLGA-DDAB/DNA in PGM and

found that their transport rates were much higher (~ 10 -fold) than that of slightly smaller COOH-PS nanoparticles. It is possible for larger particles (such as the PLGA-DDAB/DNA particles) to move more rapidly through a porous media than smaller particles by, for example, altering the pore network of the mucus or by spending less time on average either physically trapped within cages formed by elastic mucus fibers or, perhaps more likely, adherent to mucus fibers. Regardless, rapid transport through mucus and the ability to transfect cells make PLGA-DDAB/DNA particles interesting for further in vitro and in vivo testing as gene delivery agents.

Acknowledgment

The authors acknowledge Tom Kole and Yiider Tseng for technical assistance with multiple particle tracking and Junghae Suh, Stephanie Kim, and Dave McGovern for technical assistance. The authors acknowledge financial support from the National Science Foundation (CTS0210718) and the Whitaker Foundation (RG-99-0046) and fellowship funding from the National Science Foundation, the Ford Foundation, and ARCS.

References and Notes

- (1) Singh, M.; Briones, M.; Ott, G.; O'Hagan, D. Cationic microparticles: A potent delivery system for DNA vaccines. *Proc. Natl. Acad. Sci. U.S.A.* **2000**, *97*, 811–816.
- (2) Singh, M.; Ott, G.; Kazzaz, J.; Ugozzoli, M.; Briones, M. et al. Cationic microparticles are an effective delivery system for immune stimulatory CpG DNA. *Pharm. Res.* **2001**, *18*, 1476–1479.
- (3) Singh, M.; Vajdy, M.; Gardner, J.; Briones, M.; O'Hagan, D. Mucosal immunization with HIV-1 gag DNA on cationic microparticles prolongs gene expression and enhances local and systemic immunity. *Vaccine* **2001**, *20*, 594–602.
- (4) McGhee, J. R.; Lamm, M. E.; Strober, W. Mucosal immune responsees. In *Mucosal Immunology*, 2nd ed.; Academic Press: San Diego, 1999; pp 485–506.
- (5) Hanes, J.; Dawson, M.; Har-el, Y.; Suh, J.; Fiegel, J. Gene therapy in the lung. In *Pharmaceutical Inhalation Aerosol Technology*, 2nd ed.; Marcel Dekker Inc.: New York, 2003; pp 489–539.
- (6) Kumar, M.; Behera, A. K.; Lockett, R. F.; Zhang, J.; Bhullar, G. et al. Intranasal gene transfer by chitosan-DNA nanoparticles protects BALB/c mice against acute respiratory syncytial virus infection. *Hum. Gene Ther.* **2002**, *13*, 1415–1425.
- (7) Khanvilkar, K.; Donovan, M. D.; Flanagan, D. R. Drug transfer through mucus. *Adv. Drug Deliv. Rev.* **2001**, *48*, 173–193.
- (8) Saltzman, W. M.; Radomsky, M. L.; Whaley, K. J.; Cone, R. A. Antibody diffusion in human cervical mucus. *Biophys. J.* **1994**, *66*, 508–515.
- (9) Sanders, N. N.; De Smedt, S. C.; Van Rompaey, E.; Simoons, P.; De Baets, F. et al. Cystic fibrosis sputum: a barrier to the transport of nanospheres. *Am. J. Respir. Crit. Care Med.* **2000**, *162*, 1905–1911.
- (10) Olmsted, S. S.; Padgett, J. L.; Yudin, A. I.; Whaley, K. J.; Moench, T. R. et al. Diffusion of macromolecules and virus-like particles in human cervical mucus. *Biophys. J.* **2001**, *81*, 1930–1937.
- (11) Cone, R. A. Mucus. In *Mucosal Immunology*, 2nd ed.; Academic Press: San Diego, CA, 1999; pp 43–64.
- (12) Miller, J. Assay of B-galactosidase. In *Experiments in Molecular Genetics*; Miller, J., Ed.; Cold Spring Harbor Laboratory: Cold Spring Harbor, 1972; pp 352–355.
- (13) Tseng, Y.; Fedorov, E.; McCaffery, J. M.; Almo, S. C.; Wirtz, D. Micromechanics and ultrastructure of actin filament networks cross-linked by human fascin: a comparison with alpha-actinin. *J. Mol. Biol.* **2001**, *310*, 351–366.
- (14) Dawson, M.; Wirtz, D.; Hanes, J. Enhanced viscoelasticity of human cystic fibrotic sputum correlates with increasing

- microheterogeneity in particle transport. *J. Biol. Chem.* **2003**, *278*, 50393–50401.
- (15) Apgar, J.; Tseng, Y.; Fedorov, E.; Herwig, M. B.; Almo, S. C. et al. Multiple-particle tracking measurements of heterogeneities in solutions of actin filaments and actin bundles. *Biophys. J.* **2000**, *79*, 1095–1106.
- (16) Tseng, Y.; Wirtz, D. Mechanics and multiple-particle tracking microheterogeneity of alpha-actinin-cross-linked actin filament networks. *Biophys. J.* **2001**, *81*, 1643–1656.
- (17) Denis-Mize, K. S.; Dupuis, M.; MacKichan, M. L.; Singh, M.; Doe, B. et al. Plasmid DNA adsorbed onto cationic microparticles mediates target gene expression and antigen presentation by dendritic cells. *Gene Ther.* **2000**, *7*, 2105–2112.
- (18) Ferrari, S.; Kitson, C.; Farley, R.; Steel, R.; Marriott, C. et al. Mucus altering agents as adjuncts for nonviral gene transfer to airway epithelium. *Gene Ther.* **2001**, *8*, 1380–1386.
- (19) Yonemitsu, Y.; Kitson, C.; Ferrari, S.; Farley, R.; Griesenbach, U. et al. Efficient gene transfer to airway epithelium using recombinant Sendai virus. *Nat. Biotechnol.* **2000**, *18*, 970–973.
- (20) Quraishi, M. S.; Jones, N. S.; Mason, J. The rheology of nasal mucus: a review. *Clin. Otolaryngol.* **1998**, *23*, 403–413.
- (21) Rogunova, M. A.; Blackwell, J.; Jamieson, A. M.; Pasumathy, M.; Gerken, T. A. Effects of lipid on the structure and rheology of gels formed by canine submaxillary mucin. *Biorheology* **1997**, *34*, 295–308.
- (22) Norris, D.; Sinko, P. Effect of size, surface charge, and hydrophobicity on the translocation of polystyrene microspheres through gastrointestinal mucin. *J. Appl. Polym. Sci.* **1997**, *63*, 1481–1492.
- (23) Suh, J.; Wirtz, D.; Hanes, J. Efficient active transport of gene nanocarriers to the cell nucleus. *Proc. Natl. Acad. Sci. U.S.A.* **2003**, *100*, 3878–3882.

Accepted for publication January 7, 2004.

BP0342553